C–H Oxidation

Deutsche Ausgabe: DOI: 10.1002/ange.201508372
Internationale Ausgabe: DOI: 10.1002/anie.201508372

O_2 Activation and Double C–H Oxidation by a Mononuclear Manganese(II) Complex

*Claire Deville, Sandeep K. Padamati, Jonas Sundberg, Vickie McKee, Wesley R. Browne, and Christine J. McKenzie**

Abstract: *A Mn^{II} complex, $[Mn(dpeo)_2]^{2+}$ (dpeo = 1,2-di(pyridin-2-yl)ethanone oxime), activates O_2, with ensuing stepwise oxidation of the methylene group in the ligands providing an alkoxide and ultimately a ketone group. X-ray crystal-structure analysis of an intermediate homoleptic alkoxide Mn^{III} complex shows tridentate binding of the ligand via the two pyridyl groups and the newly installed alkoxide moiety, with the oxime group no longer coordinated. The structure of a Mn^{II} complex of the final ketone ligand, cis-$[MnBr_2(hidpe)_2]$ (hidpe = 2-(hydroxyimino)-1,2-di(pyridine-2-yl)ethanone) shows that bidentate oxime/pyridine coordination has been resumed. $H_2{}^{18}O$ and ${}^{18}O_2$ labeling experiments suggest that the inserted O atoms originate from two different O_2 molecules. The progress of the oxygenation was monitored through changes in the resonance-enhanced Raman bands of the oxime unit.*

The activation of molecular oxygen for the oxidation of organic substrates, despite being kinetically challenging, is carried out by a myriad of metalloenzymes[1] (with methane monooxygenase[2] perhaps being the prime example) with an ease and selectivity that is still beyond the reach of synthetic molecular transition-metal catalysts. The oxidation of C–H bonds with O_2 catalyzed by bioessential metal-based enzymes is central to elucidating enzymatic mechanisms and for the utilization of this abundant and benign resource. During photosynthesis, O–O bond formation is catalyzed by the $CaMn_4$ cluster of the oxygen-evolving center of PSII.[3] The disproportionation of H_2O_2 and the dismutation of superoxide is performed by Mn catalases and dismutases, respectively.[4] These systems often engage in O_2 release from high-valent Mn species. The reverse reaction, that is, O_2 reduction by low-valent Mn species, should be feasible.

Despite their central role in biological O_2 metabolism, our understanding of the mechanisms involved in the Mn-catalyzed activation of O_2 lags behind the spectroscopically more accessible iron- and copper-based enzymes. The spectroscopic and structural characterization of intermediates and products before and after O–O bond cleavage is therefore key to unravelling the mechanisms by which O_2 is activated. Borovik and co-workers reported a Mn complex of a urea-based tripodal ligand that forms a monomeric Mn^{III} peroxide from oxygen in the presence of reductants.[5] More recently, Kovacs and co-workers reported an unsupported mono-oxo bridge in a Mn^{III} dimer derived from O_2[6] and isolated a dimeric Mn^{III} peroxido-bridged intermediate.[7] The catalytic reduction of O_2 to H_2O_2 by a manganese thiolate complex via an intermediate mono-μ-hydroxo-bridged Mn^{III} dimer was demonstrated by Duboc and co-workers.[8] The next step in elucidating the mechanisms for the activation of molecular O_2 requires examples of highly selective oxidations, and in particular C–H oxidation. Whereas there are several reports on iron-based complexes,[9] examples with Mn have remained rare.[10] C–H oxidation at benzylic positions is known to occur in the presence of Mn and H_2O_2,[11] and some reactive intermediates have been spectroscopically observed at low temperatures.[12]

Herein, we report the first example of selective O_2 activation for C–H oxidation by a manganese complex. Exposure of the Mn^{II} complex of 1,2-di(pyridin-2-yl)ethanone oxime (dpeo, Scheme 1) to O_2 results in the selective and progressive oxygenation of the methylene group of dpeo to yield the Mn^{III} and Mn^{II} complexes, respectively, of two- and four-electron-oxidized (and oxygenated) 2-hydroxo-1,2-di(pyridine-2-yl)ethanone oxime ($hdpeo^-$) and 2-(hydroxyimino)-1,2-di(pyridine-2-yl)ethanone (hidpe, Scheme 1). We demonstrate that the initial reaction between $[Mn(dpeo)_2$-

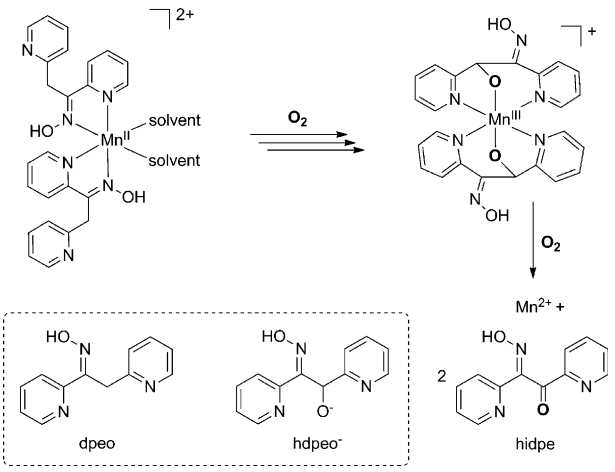

Scheme 1. Stepwise oxidation of the ligands in $[Mn^{II}(dpeo)_2(solvent)_2]^{2+}$ to $[Mn^{III}(hdpeo)_2]^+$ to ultimately produce hidpe, together with the structures of the ligands dpeo, $hdpeo^-$, and hidpe.

[*] Dr. C. Deville, Dr. J. Sundberg, Prof. Dr. V. McKee, Prof. Dr. C. J. McKenzie
Department of Physics, Chemistry and Pharmacy
University of Southern Denmark
Campusvej 55, 5230 Odense M (Denmark)
E-mail: mckenzie@sdu.dk
S. K. Padamati, Prof. Dr. W. R. Browne
Molecular Inorganic Chemistry, Stratingh Institute for Chemistry
University of Groningen
Nijenborgh 4, 9747 AG Groningen (The Netherlands)

Supporting information for this article is available on the WWW under http://dx.doi.org/10.1002/anie.201508372.

$(solvent)_2]^{2+}$ and O_2 is rapid and that the oxygen atoms incorporated into the ligand are derived solely from O_2.

The crystalline pale brown complex $[MnBr_2(dpeo)_2]$ was obtained by the reaction of $MnBr_2$ with two equivalents of dpeo in acetonitrile in air (Figure 1). This complex contains two *cis* bromides in place of the solvent molecules in the

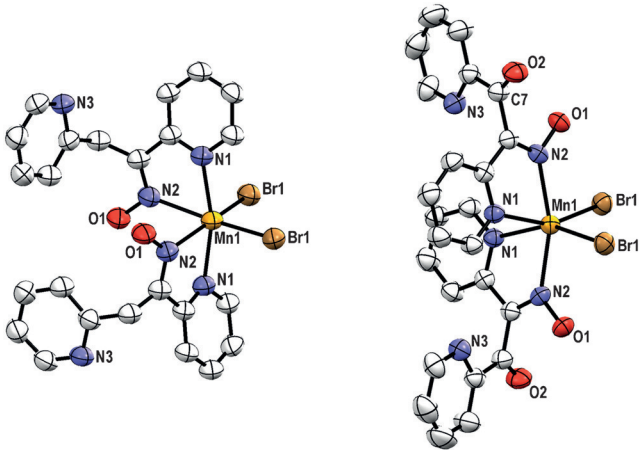

Figure 1. Single-crystal X-ray structures of $[MnBr_2(dpeo)_2]$ (left; Mn1–Br1 2.5916(11), Mn1–N1 2.225(5), Mn1–N2 2.360(5) Å) and $[MnBr_2(hidpe)_2]$ (right; Mn1–Br1 2.5948(5), Mn1–N1 2.293(2), Mn1–N2 2.237(2), C7–O2 1.210(4) Å). Ellipsoids set at 50% probability. H atoms not shown.

proposed solvated starting material in Scheme 1. This complex is a minor product (ca. 10–40%) whose occurrence is associated with rapid precipitation as crystals of this complex were located on the upper sides of the vessel and not surrounded by mother liquor. From the same reaction mixture, the yellow Mn^{II} bromide complex of the fully oxidized ligand, $[MnBr_2(hidpe)_2]$, co-crystallized. For both complexes, the ligands form a five-membered chelate to Mn^{II} through one pyridine N atom and the oxime N atom. The oxime N atoms lie in the same plane as the bromide ions and are *cis* to each other in $[MnBr_2(dpeo)_2]$, whereas in $[MnBr_2(hidpe)_2]$, they are *trans*. The C7–O2 bond length (1.208(4) Å) in $[MnBr_2(hidpe)_2]$ and the strong absorption at 1700 cm^{-1} (Supporting Information, Figure S14) are consistent with a carbonyl group. These solids are unsolvated, and the non-coordinated pyridine groups engage in intermolecular interactions (Figures S2, S3, S5, and S6).

Spontaneous oxygenation of the ligand dpeo does not occur in the absence of Mn^{2+} or in the presence of equivalent amounts of Fe^{2+}, Ni^{2+}, or Zn^{2+}. At each of the two methylene C–H sites of $[Mn(dpeo)_2(solvent)_2]^{2+}$, this oxidation is a four-electron process. In an effort to trap possible Mn–O_2 adducts, the reactions were performed in the absence of bromide. Spectroscopically distinct transient species could be observed in the reactions of $Mn^{II}(ClO_4)_2$ with dpeo (Figure 2). At room temperature, solutions containing 1:2 Mn^{II}/dpeo ($[Mn^{2+}] =$ 20 mM) turned dark brown over several hours in alcohols and in acetonitrile, which is consistent with oxidation of Mn^{II}. This was confirmed by the disappearance of the ESR signal associated with the presence of Mn^{II} (Figure S27). After one

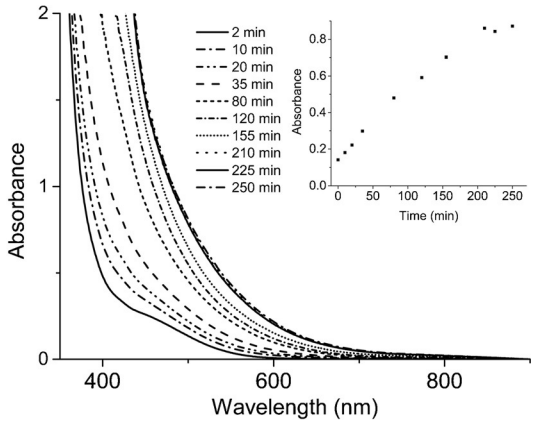

Figure 2. Changes in the UV/Vis absorption spectrum associated with Mn^{II} to Mn^{III} oxidation for a mixture of $Mn(ClO_4)_2$ (20 mM) and dpeo (40 mM) in ethanol/acetonitrile (3:1 v/v) over time. Inset: Absorbance at 500 nm.

to two days, the solutions became paler. Reactions with a Mn^{2+} concentration of at least 30 mM in ethanol/ethyl acetate (1:1) yielded precipitates of various brown hues from open vessels over hours. When the vessel was left semi-covered to slow down the rate of evaporation, no precipitation occurred, and a crystalline product was formed in approximately 20% yield. In the absence of ethyl acetate or when the reaction was performed in pure acetonitrile, no crystals were obtained. Comparison of the IR spectra of these crystals with those of the bulk precipitates show differences, suggesting the presence of structurally distinct Mn compounds. The ESI mass spectrum of the filtrate after recovery of the crystals shows almost exclusively a signal at *m*/*z* 250.06, which is due to $[Na(hidpe)]^+$ (Figure S25). The crystal structure of the light brown crystals indicates that they consist of the Mn^{III} complex of the semi-oxidized ligand, $[Mn(hdpeo)_2](ClO_4)$ (Figure 3). The structure is complicated by disorder. The C–O bond lengths of 1.425(9) Å for the major component and 1.408(11) Å for a minor disorder component are consistent with a C–O single bond and are about 0.2 Å greater than the C=O bonds in $[MnBr_2(hidpe)_2]$. The

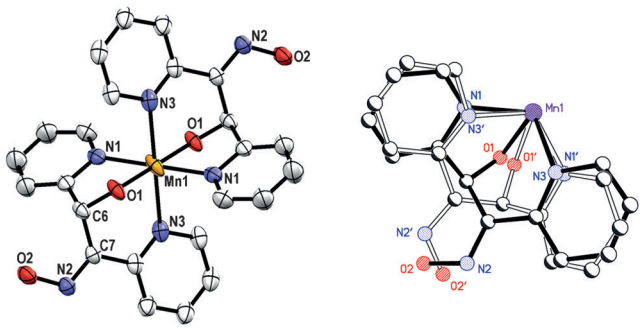

Figure 3. Left: Centrosymmetric cation of the major component (57.5%) of $[Mn(hdpeo)_2](ClO_4)$, with the ellipsoids set at 50% probability (Mn1–O1 1.854(9), Mn1–N1 2.143(15), Mn1–N3 2.237(15) Å). H atoms not shown. Right: Asymmetric unit of the cation showing disorder. White bonds and atoms labeled with indicate the minor component (42.5%).

centrosymmetric cation of the major component is shown in Figure 3. The Mn^{III} cation lies on a center of symmetry and is coordinated to two tridentate anionic ligands via the pyridine nitrogen atoms and the new alkoxide oxygen atoms. The $hdpeo^-$ ligand is facially coordinated but disordered with the other enantiomer (the ligand is chiral at C6). The positions of the donor atoms in the two components overlap closely, although the sites of the pyridine rings containing N1 and N3 are exchanged (Figure 3). The bond lengths confirm the presence of a C=N oxime group (C7–N2 1.287(7) and 1.295(10) Å for the major and minor components, respectively). Further structural details can be found in the Supporting Information.

When the isolated $[Mn(hdpeo)_2]^+$ complex was redissolved, the ligand underwent further oxidation to the ketone in the presence of O_2, albeit at a much slower rate than for the initial oxygenation (1–2 days). The ESI mass spectrum of $[Mn(hdpeo)_2](ClO_4)$ that was recorded immediately after dissolution, shows a peak at *m*/*z* 511.09, which is consistent with $[Mn(hdpeo)_2]^+$. Upon standing for several days, ions associated with the formation of hidpe ($[Na(hidpe)]^+$ at *m*/*z* 250.06) were observed, and an ESR signal associated with the presence of Mn^{II} reappeared (Figure S28). Mixtures of $Mn^{II}(ClO_4)_2$ and dpeo kept under nitrogen atmosphere are yellow, and the main signals observed by ESIMS are found at *m*/*z* 214.10 ($dpeoH^+$) and 236.08 ($[Na(dpeo)]^+$), together with signals assigned to $[Mn(dpeo)(dpeo-H)]^+$ (*m*/*z* 480.11), $[Mn(dpeo)_2(ClO_4)]^+$ (*m*/*z* 580.07), and a very weak signal assigned to $[Mn(dpeo)_2(dpeo-H)]^+$ (*m*/*z* 693.20; Figure S26). These signals are absent in the aerated solutions from which $[Mn(hdpeo)_2](ClO_4)$ was isolated in crystalline form (Figures S24 and S25).

Data from the reactions performed in the presence of either $^{18}O_2/H_2O$ or $O_2/H_2{}^{18}O$ confirmed that the source of the O atoms in $hdpeo^-$ and hidpe is O_2. ESI mass spectra of the solids obtained from reactions containing $H_2{}^{18}O$ after 72 hours show a signal for unlabeled $[Mn(hdpeo)_2]^+$ at *m*/*z* 511.09 (calculated: *m*/*z* 511.09), whereas with $^{18}O_2$, only a signal at *m*/*z* 515.10 was observed, confirming the sole formation of $[Mn([^{18}O]\text{-}hdpeo)_2]^+$ (Figure 4). ESI mass spectra of solutions exposed to a limiting 1:1 mixture of $^{18}O_2$ and $^{16}O_2$ show signals for the unoxidized dpeo ligand and the bis(dpeo)Mn^{II} and bis(hdpeo)Mn^{III} complexes. For the latter, an approximately 1:2:1 mixture of $[Mn([^{16}O]\text{-}hdpeo)_2]^+$, $[Mn([^{16}O]\text{-}hdpeo)([^{18}O]\text{-}hdpeo)]^+$, and $[Mn([^{18}O]\text{-}hdpeo)_2]^+$ at *m*/*z* 511.09, 513.10, and 515.10 was observed (Figures S21–S23). This result suggests that each inserted O atom originates from a different O_2 molecule. Weak, but nonetheless potentially mechanistically significant, signals corresponding to the heteroleptic complexes $[Mn(dpeo)([^{16}O]\text{-}hdpeo)]^+$ and $[Mn(dpeo)([^{18}O]\text{-}hdpeo)]^+$ were also observed.

During the reaction between Mn^{II} and dpeo, the absorbance in the near-UV region increases substantially, providing an opportunity to monitor the formation of various species by resonance Raman spectroscopy. Enhancement of the otherwise weak Raman spectrum of the ligand dpeo was possible at the concentrations of typical reactions (0.25 to 40 mM) with excitation at 355 nm. The spectra of mixtures of dpeo and $Mn(ClO_4)_2$ (in ratios of 1:0.15 to 1:1) indicate that 0.5 equivalents of Mn^{II} per dpeo are sufficient to obtain full conversion into $hdpeo^-$. This is manifested in the disappearance of the dpeo band at 1523 cm^{-1} within several minutes that was observed unless there were less than 0.5 equivalents of Mn^{II} present (Figure S16). The rate of reaction in dilute solutions (i.e., when the concentration of the O_2 is not limiting) suggests that the O_2-activating species is $[Mn(dpeo)_2]^{2+}$. Unreacted coordinated dpeo, indicated by the absorption at 1523 cm^{-1}, disappeared from mixtures containing the metal and ligand in ratios of up to 1:6 within 15 hours. This conversion indicates that dpeo oxidation to the ketone, hidpe, is catalytic in Mn^{II} (Scheme 2).

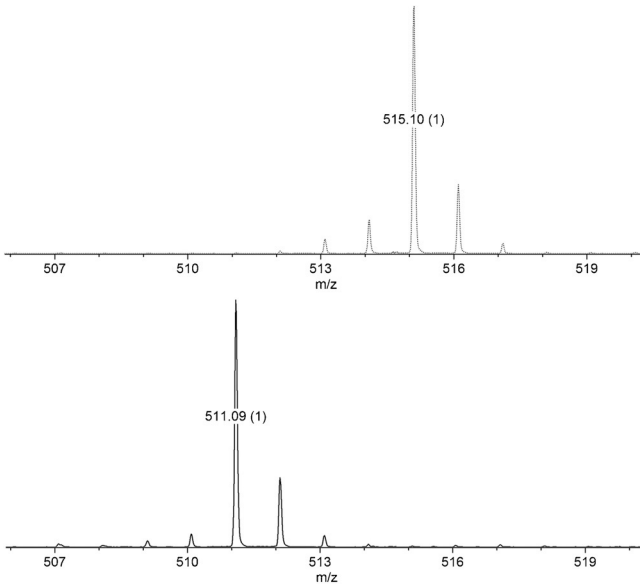

Figure 4. Sections of the ESI mass spectra of the isolated complexes $[Mn^{III}(hdpeo)_2](ClO_4)$ (bottom) and $[Mn^{III}([^{18}O]\text{-}hdpeo)_2](ClO_4)$ (top) in acetonitrile. For the full spectra, see Figures S19–S20.

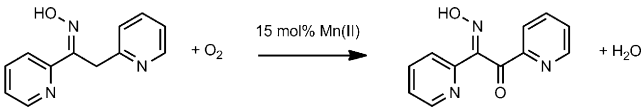

Scheme 2. Catalytic oxidation of dpeo to hidpe.

The formation of a dpeo complex with $Mn(ClO_4)_2$ and its subsequent oxidation with O_2 was monitored under O_2 limiting conditions, that is, $[O_2] < [dpeo]$ and $[O_2] < [Mn^{II}]$. The resonance-enhanced band attributed to the imine group of the hydroxylamine moiety of coordinated dpeo at 1523 cm^{-1} decreased in intensity with a concomitant increase in the band at 1548 cm^{-1} (Figure 5). A weak, unassigned band at 709 cm^{-1} (not shown) appeared over 30 minutes.

On the basis of 1) the 2:1 dpeo/$Mn(ClO_4)_2$ reaction, 2) the apparent 1:1 $[Mn(dpeo)_2]^{2+}/O_2$ stoichiometry, 3) the rate of the initial oxidation under dilute conditions, and 4) the fact that the two O atoms incorporated into $[Mn(hdpeo)_2]^+$ do not seem to be derived from the same molecule of O_2, we propose

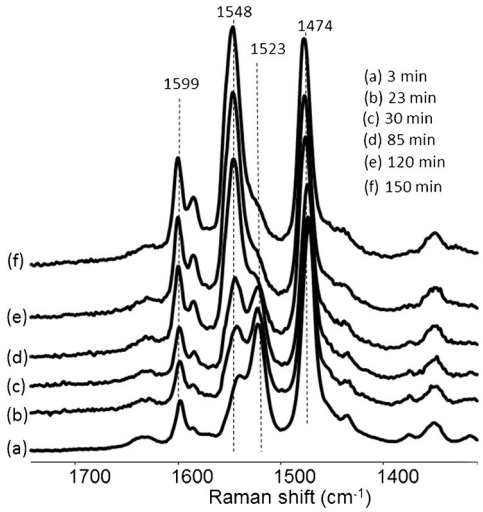

Figure 5. Resonance Raman spectra (λ_{ex} = 355 nm) of a 2:1 mixture of $Mn(ClO_4)_2$ (20 mM) and dpeo (40 mM) in acetonitrile/ethanol (25:75). For the full spectra, see Figure S18. The first spectrum obtained immediately after mixing Mn^{II} with dpeo is predominantly that of $[Mn(dpeo)_2(solvent)_2]^{2+}$ (Figure S15). All spectra were normalized to the 881 cm^{-1} band of the solvent.

a mechanism for O_2 activation by Mn^{II} and the ensuing two-step ligand/substrate C–H oxidation (Scheme 3). Mn^{III} superoxo and Mn^{IV} oxo species act as H atom abstractors. The accessibility of two different metal-based oxidants is reasonable for homogenous manganese catalysts.[13] It is pertinent to note that the system furnishes the possibility of H atom relay pathways facilitated by the second coordination sphere via the vicinal oxime and pyridine groups. These processes might be benefit from substrate coordination via the pyridine bearing the target C–H group in its α-position, as depicted specifically for the oxidation step promoted by the Mn^{IV} oxo species. Raman spectral data show that complexation of Mn^{II} with dpeo occurs immediately upon mixing, which increases the driving force for the binding of O_2 with concomitant oxidation of Mn^{II} to form a Mn^{III} superoxide species. Intramolecular hydrogen atom abstraction from the ligand by the metal(III)-bound superoxide[14] followed by O–O bond cleavage must occur in concert with oxidation of the ligand/substrate C–H bond owing to the incorporation of oxygen atoms from O_2.

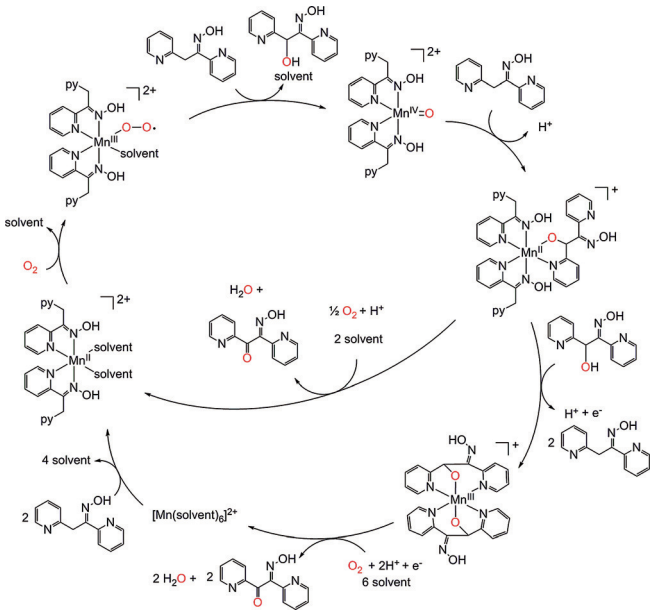

Scheme 3. Proposed reaction mechanism.

In summary, a mononuclear Mn^{II} complex of the new ligand 1,2-di(pyridin-2-yl)-ethanone oxime (dpeo) has been shown to activate O_2. This process results in the oxygenation of the methylene C–H bond α to the 2-pyridyl group to give an alkoxide and subsequently the ketone derivative in a stepwise fashion. The Mn^{III} and Mn^{II} complexes of the alkoxide and ketone ligand derivatives, respectively, were characterized by single-crystal X-ray crystallography. The alkoxide complex is metastable. When $[Mn(hdpeo)_2](ClO_4)$ was redissolved, the oxidation of the ligand continued to finally give the ketone. When the reaction was performed with 99 % $^{18}O_2$, both ligands in the bis(hdpeo) complexes were labeled; however, the O atoms in the two ligands do not originate from the same O_2 molecule. Raman spectroscopy and experiments in which the ligand/Mn^{II} ratio was varied confirmed that the initial reaction of $[Mn(dpeo)_2]^{2+}$ with O_2 is fast, and that the undetected initial adduct is mononuclear. Protection of the benzylic position in this system may open a new strategy for the design of manganese-based O_2 activating catalysts.

Acknowledgements

This work was supported by the Danish Council for Independent Research | Natural Sciences (4181-00329 to C.McK.), the Villum Foundation (post-doctoral funding for C.D.), the Velux foundation (visiting professorship to V.McK.), the European Research Council (ERC-2011-StG-279549 to S.K.P. and W.R.B.), and the Ministry of Education, Culture and Science (Gravity program 024.001.035, W.R.B.). The COST action CM1003 is acknowledged for financial support (STSM-CM1003-260115-054197 to C.D.). We thank Mie Thorborg Pedersen for preparing the front cover image.

Keywords: catalysis · C–H oxidation · manganese · O_2 activation · oxime ligands

How to cite: *Angew. Chem. Int. Ed.* **2016**, *55*, 545–549
Angew. Chem. **2016**, *128*, 555–559

[1] a) I. Ivanov, D. Heydeck, K. Hofheinz, J. Roffeis, V. B. O'Donnell, H. Kuhn, M. Walther, *Arch. Biochem. Biophys.* **2010**, *503*, 161–174; b) A. Andreou, I. Feussner, *Phytochemistry* **2009**, *70*, 1504–1510; c) P. Brzezinski, R. B. Gennis, *J. Bioenerg. Biomembr.* **2008**, *40*, 521–531; d) M. Brunori, A. Giuffrè, P. Sarti, *J. Inorg. Biochem.* **2005**, *99*, 324–336; e) M. M. E. Huijbers, S. Montersino, A. H. Westphal, D. Tischler, W. J. H. van Berkel, *Arch. Biochem. Biophys.* **2014**, *544*, 2–17; f) E. I. Solomon,

U. M. Sundaram, T. E. Machonkin, *Chem. Rev.* **1996**, *96*, 2563 – 2605; g) L. Quintanar, C. Stoj, A. B. Taylor, P. J. Hart, D. J. Kosman, E. I. Solomon, *Acc. Chem. Res.* **2007**, *40*, 445 – 452.

[2] a) M. A. Culpepper, A. C. Rosenzweig, *Crit. Rev. Biochem. Mol. Biol.* **2012**, *47*, 483 – 492; b) S. Sirajuddin, A. C. Rosenzweig, *Biochemistry* **2015**, *54*, 2283 – 2294; c) R. L. Lieberman, A. C. Rosenzweig, *Nature* **2005**, *434*, 177 – 182.

[3] a) Y. Umena, K. Kawakami, J.-R. Shen, N. Kamiya, *Nature* **2011**, *473*, 55 – 61; b) J. P. McEvoy, G. W. Brudvig, *Chem. Rev.* **2006**, *106*, 4455 – 4483.

[4] N. A. Law, M. T. Caudle, V. L. Pecoraro, *Adv. Inorg. Chem.* **1998**, *46*, 305 – 440.

[5] a) R. L. Shook, W. A. Gunderson, J. Greaves, J. W. Ziller, M. P. Hendrich, A. S. Borovik, *J. Am. Chem. Soc.* **2008**, *130*, 8888 – 8889; b) Y. J. Park, J. W. Ziller, A. S. Borovik, *J. Am. Chem. Soc.* **2011**, *133*, 9258 – 9261; c) R. L. Shook, S. M. Peterson, J. Greaves, C. Moore, A. L. Rheingold, A. S. Borovik, *J. Am. Chem. Soc.* **2011**, *133*, 5810 – 5817.

[6] M. K. Coggins, L. M. Brines, J. A. Kovacs, *Inorg. Chem.* **2013**, *52*, 12383 – 12393.

[7] a) M. K. Coggins, X. Sun, Y. Kwak, E. I. Solomon, E. Rybak-Akimova, J. A. Kovacs, *J. Am. Chem. Soc.* **2013**, *135*, 5631 – 5640; b) J. A. Rees, V. Martin-Diaconescu, J. A. Kovacs, S. DeBeer, *Inorg. Chem.* **2015**, *54*, 6410 – 6422.

[8] M. Gennari, D. Brazzolotto, J. Pécau, M. V. Cherrie, C. J. Pollock, S. DeBeer, M. Retegan, D. A. Pantazis, F. Neese, M. Rouzières, R. Clérac, C. Duboc, *J. Am. Chem. Soc.* **2015**, *137*, 8644 – 8653.

[9] a) "Iron Catalysis II": D. P. de Sousa, C. J. McKenzie in *Topics in Organometallic Chemistry, Vol. 50* (Ed.: E. Bauer), Springer, Berlin, **2015**; b) A. Nielsen, F. B. Larsen, A. D. Bond, C. J. McKenzie, *Angew. Chem. Int. Ed.* **2006**, *45*, 1602 – 1606; *Angew. Chem.* **2006**, *118*, 1632 – 1636; c) Y.-M. Lee, S. Hong, Y. Morimoto, W. Shin, S. Fukuzumi, W. Nam, *J. Am. Chem. Soc.* **2010**, *132*, 10668 – 10670; d) E. H. Ha, R. Y. N. Ho, J. F. Kisiel, J. Selverstone Valentine, *Inorg. Chem.* **1995**, *34*, 2265 – 2266; e) M. P. Mehn, K. Fujisawa, E. L. Hegg, L. Que, Jr., *J. Am. Chem. Soc.* **2003**, *125*, 7828 – 7842; f) A. Mukherjee, M. Martinho, E. L. Bominaar, E. Münck, L. Que, Jr., *Angew. Chem. Int. Ed.* **2009**, *48*, 1780 – 1783; *Angew. Chem.* **2009**, *121*, 1812 – 1815; g) H. Jaafar, B. Vileno, A. Thibon, D. Mandon, *Dalton Trans.* **2011**, *40*, 92 – 106; h) Y. He, C. R. Goldsmith, *Chem. Commun.* **2012**, *48*, 10532 – 10534.

[10] G. B. Wijeratne, B. Corzine, V. W. Day, T. A. Jackson, *Inorg. Chem.* **2014**, *53*, 7622 – 7634.

[11] D. Pijper, P. Saisaha, J. W. de Boer, R. Hoen, C. Smit, A. Meetsma, R. Hage, R. P. van Summeren, P. L. Alsters, B. L. Feringa, W. R. Browne, *Dalton Trans.* **2010**, *39*, 10375 – 10381.

[12] S. Groni, P. Dorlet, G. Blain, S. Bourcier, R. Guillot, E. Anxolabéhère-Mallart, *Inorg. Chem.* **2008**, *47*, 3166 – 3172.

[13] a) C. Deville, M. Finsel, D. P. de Sousa, B. Szafranowska, J. Behnken, S. Svane, A. D. Bond, R. K. Seidler-Egdal, C. J. McKenzie, *Eur. J. Inorg. Chem.* **2015**, *21*, 3485 – 3492; b) W. M. C. Sameera, C. J. McKenzie, J. E. McGrady, *Dalton Trans.* **2011**, *40*, 3859 – 3870.

[14] M. S. Vad, A. Nielsen, A. Lennartson, A. D. Bond, J. E. McGrady, C. J. McKenzie, *Dalton Trans.* **2011**, *40*, 10698 – 10707.

Received: September 7, 2015
Revised: October 14, 2015
Published online: December 3, 2015

